Abdallah BELABBES[1], Anouar LAIDANI[2], Amina YACHIR[3], Allal El Moubarek BOUZID[4], Riyadh BOUDDOU[5], Omar Abdelaziz LITIM[2]

University of Science and Technology MB, Laboratory of Vision Automation and Intelligent Control Systems AVCIS Oran, Algeria (1)
University of Oran 2 Mohammed Ben Ahmed, Industrial maintenance and safety institute, Oran, Algeria (2)
National Polytechnic School, Laboratory of Automation and Systems Analysis LAAS, Oran, Algeria (3)
Icam, Site de Toulouse, Toulouse, France (4)
Department of Electrical Engineering, Institute of Technology, University Center of Naama, Algeria (5)
ORCID: 1. 0000-0003-0072-6883; 4. 0000-0003-4623-1923; 5. 0000-0001-6555-5785

doi:10.15199/48.2024.02.02

Advanced Control of PMSG-based Wind Energy Conversion System Using Model Predictive and Sliding Mode Control

Abstract. *This paper proposes a sliding mode control (SMC) and a model predictive control (MPC) for controlling a PMSG wind turbine. The MPC forces the system to follow the defined sliding surface. The major advantages of SMC are robustness, fast response, and simple implementation, but one of the inconveniences is chattering. Therefore, the MPC has been proposed in this paper which uses the mathematical model of the system to predict the possible future behaviour of the controlled variables, and this technique allows the selection of the optimal voltage vector that leads to minimum error using a cost function which leads to low maintenance costs and low total harmonic distortion in current.*

Streszczenie. *W artykule zaproponowano sterowanie w trybie ślizgowym (SMC) i sterowanie predykcyjne modelu (MPC) do sterowania turbiną wiatrową PMSG. MPC zmusza system do podążania za zdefiniowaną powierzchnią ślizgową. Głównymi zaletami SMC są solidność, szybka reakcja i prosta implementacja, ale jedną z niedogodności jest chattering, dlatego w tym artykule zaproponowano MPC, który wykorzystuje model matematyczny systemu do przewidywania możliwego przyszłego zachowania kontrolowanych zmiennych, technika ta pozwala na wybór optymalnego wektora napięcia, który prowadzi do minimalnego błędu przy użyciu funkcji kosztu, co prowadzi do niskich kosztów utrzymania i niskich całkowitych zniekształceń harmonicznych w prądzie. (**Zaawansowane sterowanie systemem konwersji energii wiatrowej opartym na PMSG przy użyciu modelu predykcyjnego i sterowania w trybie ślizgowym**)*

Keywords: PMSG, Wind turbine, Sliding mode control, Model predictive control.
Słowa kluczowe: PMSG, turbina wiatrowa, sterowanie trybem ślizgowym, sterowanie predykcyjne modelu.

1. Introduction

There are two types of energy in the world, renewable and non-renewable energies like oil and nuclear energy. The advantage of renewable energy is that it is natural and will exist forever. Unlike non-renewable energy, it's limited, the entire world is shifting toward this energy, and wind energy is a renewable energy source. This energy is a fuel substitute and protects the environment [1]. The wind generator collects this energy and converts it into a mechanical one. Then this power is fed to a generator that converts this energy into electricity. There are different types of generators used in this turbine, like doubly-fed induction generator (DFIG), but the most much-used generator is the permanent magnet synchronous generator (PMSG). PMSG-based wind energy conversion systems (WECS) have received a great degree of interest recently because of their small structure, reduced maintenance requirements, and better efficiency and control capabilities. As a result, PMSG-WECS has developed into a leading research hotspot in wind power generation [2]. The PMSG-based WECS generates electricity, but it must be controllable to meet the following grid conditions: fixed frequency, voltage regulation, synchronisation, phase alignment, and active and reactive power control. The PMSG-based WECS will be installed on the grid through a back-to-back IGBT converter with two components linked by a DC link capacitor. IGBT converters provide the power conversion capabilities and control functions required for the efficient, grid-compliant operation of PMSG wind turbines. IGBT converters are essential for optimising wind turbine performance and grid integration [3]. PMSG-based WECS are composed of two parts, as presented in figure 1, the synchronous generator-side converter (SGSC) and the grid-side converter (GSC), and several control methods have been proposed to control the back-to-back IGBT converter. Each control has its unique features. There is classic control like Proportional-Integral-Derivative control (PID). Still, it has some limitations due to fixed control parameters (proportional, integral, and derivative gains) and needs to directly consider the specific dynamics and characteristics of the controlled system. This can lead to suboptimal performance in complex and non-linear systems. And there are advanced controls that offer more control capabilities and take into account non-linear systems, this control method can be used in a linear system, and the most often used are Field Oriented Control (FOC), Fuzzy Logic Control (FLC), SMC, and MPC [4].

SMC is designed to make the system slide around the pre-defined slide surface and stay there regardless of uncertainty and variations in operating conditions, e.g., wind speed or uncertainty in the system parameters. The system moves from one differentiator to another and is modified using a discrete set of controls to achieve the desired system behaviour [5]. In this paper, this technique is implemented on both sides of the system, as shown in figure 2 and figure 3. Although SMC offers advantages like robustness, fast response, and easy to implement, it also has disadvantages like chattering there for another advanced control has been developed to solve common SMC problems and enhance system performance. This technique is called MPC.

MPC is designed as an optimal solution for controlling the PMSG wind turbine and meeting our grid requirements. The concept of MPC is that it uses the system model to forecast the behaviour of the variables being controlled and uses a cost function to choose the voltage vector that minimizes the margin of error between the controlled variable and its reference. This new technique is also implemented on both sides of the system, as shown in figures 4 and 5. This control technique offers advantages like constraint handling, fast response, low maintenance cost, low THD current, and optimal power extraction, but it also comes with some potential inconveniences and challenges like computational complexity. MPC solves an optimization problem at each control step, for it will need a powerful processing power with large memory.

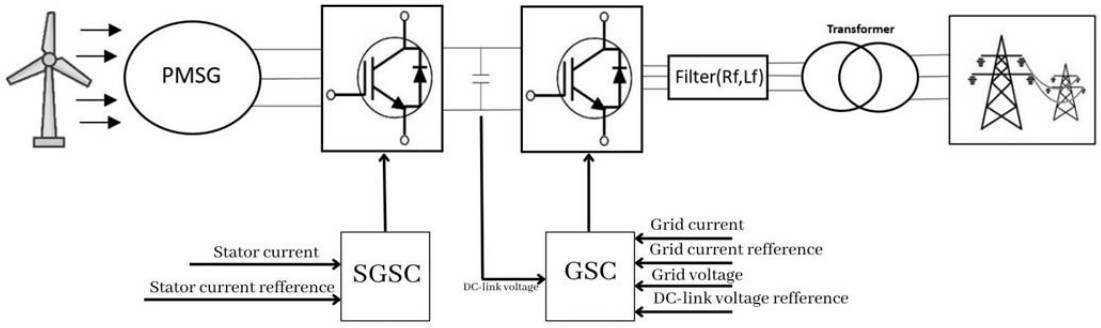

Fig.1. PMSG wind turbine system control

The aim of this work is to present the SMC and the MPC used for back-to-back IGBT converter control in the PMSG-based WECS.

This paper is structured in the following sections. Section 2 presents the mathematical model of the generator and grid side of the PMSG wind turbine, while Sections 3 and 4 deal with the sliding mode and model prediction techniques, respectively. Section 5 presents simulation results to compare and discuss the performance of the two advanced controls.

2. System modelling

2.1 Wind turbine model

The model of wind power is as follows [7]:

$$P_{wind} = \frac{1}{2}\rho \times S \times V^3 \tag{1}$$

The turbine can generate only a certain percentage of the available wind power. This percentage is represented with C_p. The wind turbine equations are as follows [7],[13]:

$$P_{turb} = \frac{1}{2} \times C_p \times \rho \times S \times V^3 \tag{2}$$

$$T_{turb} = \frac{P_{turb}}{\Omega_t} \tag{3}$$

Where C_p is the power coefficient [8]:

$$C_p = 0.5\left(\frac{116}{\lambda_i} - 0.4\beta - 5\right)e^{\frac{-21}{\lambda_i}} + 0.0068\lambda \tag{4}$$

With:

$$\frac{1}{\lambda_i} = \frac{1}{\lambda + 0.08 \times \beta} - \frac{0.035}{\beta^3 + 1} \tag{5}$$

2.2 Maximum power point tracking (MPPT)

The MPPT strategy aims to extract the maximum power from the wind turbine, i.e., to increase the power coefficient C_p. To ensure this, the electromagnetic torque needs to be estimated and controlled using the MPPT technique. The maximum power is extracted when λ_{opt}=8.1 and $\beta = 0^0$ [9]:

$$\lambda = \frac{\Omega_t \times R}{V} \tag{6}$$

$$T_{em-ref} = \frac{P_{turb-ref}}{\Omega_t} = \frac{\rho \times \pi \times R^5 \times C_{p-\max} \times \Omega_t^2}{2 \times \lambda_{opt}^3} \tag{7}$$

2.3 Synchronous generator side model

The PMSG is modelled using the d-q synchronous reference and is defined as follows [10]:

$$\frac{di_{sd}}{dt} = -\frac{R_s}{L_{sd}} i_{sd} + \frac{\omega_s L_{sq}}{L_{sd}} i_{sq} + \frac{V_{sd}}{L_{sd}} \tag{8}$$

$$\frac{di_{sq}}{dt} = -\frac{R_s}{L_{sq}} i_{sq} - \frac{\omega_s L_{sd}}{L_{sq}} i_{sd} - \frac{\omega_s \phi_f}{L_{sq}} + \frac{V_{sq}}{L_{sq}} \tag{9}$$

$$T_e = \frac{3}{2} p[(L_{sd} - L_{sq}) i_{sd} i_{sq} + \phi_f \times i_{sq}] \tag{10}$$

$$\frac{d\Omega_{mec}}{dt} = \frac{1}{J} T_{turb} - \frac{3}{2} \times \frac{p}{J} \times \phi_f i_{sq} - \frac{f}{J} \Omega_{mec} \tag{11}$$

Where i_{sd} and i_{sq} are the currents of the stator in the d-q frame, V_{sd} and V_{sq} are the stator voltage in the d-q frame, ϕ_f is the flux of the permanent magnet, ω_s is the angular rotor speed, p is the poles pairs number, f is the friction coefficient, R_s is the stator resistance, L_{sd} and L_{sq} are the stator inductances in the d-q frame, T_e is the electromagnetic torque applied to the PMSG, J is the inertia coefficient.

2.4 Grid side model

The grid-side converter model connected to a filter is described in the d-q synchronous reference as the following [10]:

$$\frac{di_{gd}}{dt} = \frac{V_{gd}}{L_f} - \frac{R_f}{L_f} i_{gd} + \omega_g i_{gq} - \frac{V_{id}}{L_f} \tag{12}$$

$$\frac{di_{gq}}{dt} = \frac{V_{gq}}{L_f} - \frac{R_f}{L_f} i_{gq} - \omega_g i_{gd} - \frac{V_{iq}}{L_f} \tag{13}$$

$$P_g = V_{gd} i_{gd} + V_{gq} i_{gq} \tag{14}$$

$$Q_g = V_{gd} i_{gd} - V_{gq} i_{gq} \tag{15}$$

Where i_{gd} and i_{gq} are the currents of the grid in the d-q frame, V_{gd} and V_{gq} are the voltage grid in the d-q frame, ω_g is the grid voltage angular frequency, V_{id} and V_{iq} are the voltage output of the converter in the d-q frame, R_f is the filter resistance, L_f is the filter inductances in the d-q frame.

3. Sliding mode control

In SMC, the control law is adapted to drive the trajectories of the system's state on a predetermined "sliding surface" in a given finite time. The sliding surface is defined based on the desired system behaviour and is constructed to make the system dynamics simple when projected onto this surface. The control law aims to maintain the system's state on this sliding surface, ensuring robustness against uncertainties and disturbances.

3.1 SMC model in synchronous generator side converter

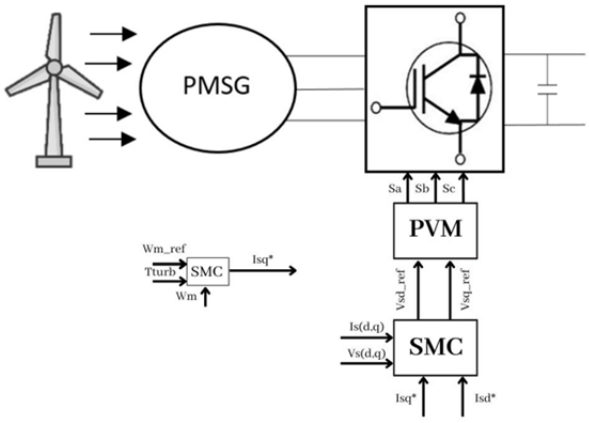

Fig.2. Generator side of PMSG wind turbine control system

Three controllers are installed using the sliding mode on this side to control the d-q axis stator current (i_{sd}, i_{sq}) and the speed (Ω_{mec}). The sliding surfaces are defined as the following [5]:

(16) $$S(i_{sd}) = e(i_{sd}) = i_{sd}^{*} - i_{sd}$$

(17) $$S(i_{sq}) = e(i_{sq}) = i_{sq}^{*} - i_{sq}$$

(18) $$S(\Omega_{mec}) = e(\Omega_{mec}) = \Omega_{mec}^{*} - \Omega_{mec}$$

Each axis control is as follows [6]:

(19) $$V_{sd_{ref}} = V_{sd_{eq}} + V_{sd_N}$$

(20) $$V_{sq_{ref}} = V_{sq_{eq}} + V_{sq_N}$$

By applying the time derivative to expressions (8,9) and taking into account that the sliding mode appears on the sliding surface if $(\dot{S}(x) = 0)$, therefor we obtain the following control equations:

(21) $$V_{sd_{eq}} = L_d\left[\frac{di_{sd}^{*}}{dt} + \frac{R_s}{L_{sd}} i_{sd} - \omega_s \frac{L_{sq}}{L_{sd}} i_{sq}\right]$$

(22)

$$V_{sq_{eq}} = L_q\left[\frac{di_{sq}^{*}}{dt} + \frac{R_s}{L_{sq}} i_{sq} + \omega_s \frac{L_{sd}}{L_{sq}} i_{sd} + \omega_s \frac{\phi_f}{L_{sq}}\right]$$

And the switching control expressions are defined as:

(23) $$V_{sd_N} = K_{gd} \times S(i_{sd}) \text{ with } K_{sd} > 0$$

(24) $$V_{sq_N} = K_{gq} \times S(i_{sq}) \text{ with } K_{sq} > 0$$

With i_{sd}^{*} and i_{sq}^{*} are the dq axis reference current of the stator, respectively, the d axis current of the stator is maintained at zero to obtain maximum torque, and the q axis stator current is controlled using the sliding mode:

(25) $$i_{sq}^{*} = i_{sq_{eq}} + i_{sq_N}$$

We apply the derivative to equation (11) to obtain the following control expression:

(26) $$i_{sq_{eq}} = -\frac{2J}{3p\phi_f}\left[\frac{d\Omega_{mec}^{*}}{dt} + \frac{f}{J}\Omega_{mec} - \frac{1}{J}T_{turb}\right]$$

The switching control expression is defined as follows:

(27) $$i_{sq_N} = K_{\Omega_{mec}} \times S(\Omega_{mec}) \text{ with } K_{\Omega_{mec}} > 0$$

Where Ω_{mec}^{*} is the mechanical speed reference.

3.2 SMC model in grid side converter

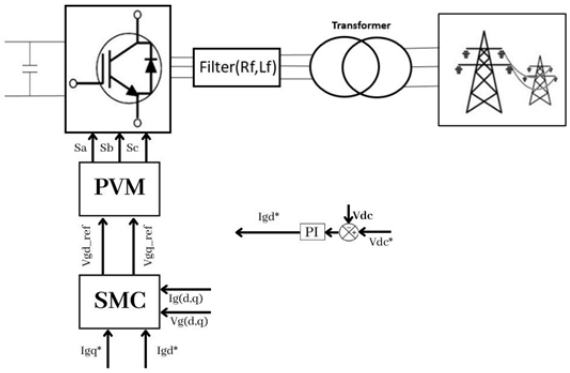

Fig.3. Grid side PMSG wind turbine control system

Using the sliding mode on this side, two controllers are installed to control the d-q axis grid current (i_{gd}, i_{gq}). The sliding surfaces are defined as follows [5]:

(28) $$S(i_{gd}) = e(i_{gd}) = i_{gd}^{*} - i_{gd}$$

(29) $$S(i_{gq}) = e(i_{gq}) = i_{gq}^{*} - i_{gq}$$

Each axis control is as follows [6]:

(30) $$V_{gd_{ref}} = V_{gd_{eq}} + V_{gd_N}$$

(31) $$V_{gq_{ref}} = V_{gq_{eq}} + V_{gq_N}$$

We apply the time derivative to expressions (12,13):

(32) $$V_{gd_{eq}} = L_f\left[\frac{di_{gd}^{*}}{dt} + \frac{R_f}{L_f} i_{gd} - \omega_g i_{gq} + \frac{V_{id}}{L_f}\right]$$

(33) $$V_{sq_{eq}} = L_f\left[\frac{di_{gq}^{*}}{dt} + \frac{R_f}{L_f} i_{gq} + \omega_g i_{gd} + \frac{V_{iq}}{L_f}\right]$$

And the switching control expressions are defined as:

(34) $$V_{gd_N} = K_{gd} \times S(i_{gd}) \text{ with } K_{gd} > 0$$

(35) $$V_{gq_N} = K_{gq} \times S(i_{gq}) \text{ with } K_{gq} > 0$$

With i_{gd}^{*} and i_{gq}^{*} are the d-q axis reference current of the grid, respectively, the d axis grid current is controlled using an external PI controller that controls the voltage measured in DC-link to track its reference at a constant value and the q axis grid current is also controlled with an external PI controller that regulates the reactive power to its reference that is fixed at zero to reach the unity power factor.

4. Model predictive control

MPC is considered an advanced control. It requires a clear insight into system behaviour and accurate system modelling. Though MPC comes with many advantages, like handling constraints, it also comes with disadvantages, like the requirement of robust processing power with large memory to solve an optimization problem at each time step. Like SMC, MPC will be implemented on both sides of the PMSG wind system [11].

4.1 MPC model in synchronous generator side converter

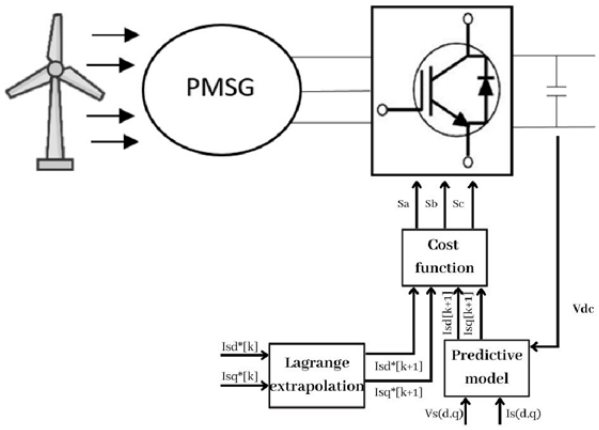

Fig.4. Generator side of PMSG wind turbine control system

MPC control of the SGSC is designed to calculate the optimum converter voltage vector to apply within the following sampling period to reduce the error between the current in the stator and its reference in the d-q framework. The reference of the d-axis stator current $i_{sd}^{*}$is kept at zero to obtain the maximum torque, while the reference of the q-axis stator current i_{sq}^{*} is achieved through an external slip-based controller. We apply the forward Euler discretization method to equations (8,9), and we obtain the following prediction equations [12]:

(36) $$i_{sd}[k+1] = a_1 i_{sd}[k] + a_2(\omega_s[k] L_{sq} i_{sq}[k] + V_{sd}[k])$$

(37) $$i_{sq}[k+1] = a_3 i_{sq}[k] + a_4(L_{sd} i_{sd}[k] + \phi_f) + a_5 V_{sd}[k]$$

Where $a_1 = \frac{1-R_s T_s}{L_{sd}}$, $a_2 = \frac{T_s}{L_{sd}}$, $a_3 = \frac{1-R_s T_s}{L_{sq}}$, $a_4 = -\frac{\omega_s T_s}{L_{sq}}$, $a_5 = \frac{T_s}{L_{sq}}$ and T_s is the sampling period. $i_{sd}[k+1]$ and $i_{sd}[k+1]$ are the stator planned current in the dq frame at the (k+1) sampling period, $i_{sd}[k]$ and $i_{sd}[k]$ are the currents of the stator in the dq frame at the (k) sampling period A cost function is then determined by the following [13]:

(38) $$g_s = \Delta i_{sd}[k+1] + \Delta i_{sq}[k+1]$$

With:

(39) $$\Delta i_{sd}[k+1] = (i_{sd}^{*}[k+1] - i_{sd}[k+1])^2$$

(40) $$\Delta i_{sq}[k+1] = (i_{sq}^{*}[k+1] - i_{sq}[k+1])^2$$

With $i_{sd}^{*}[k+1]$ and $i_{sq}^{*}[k+1]$ are the d-q axis reference current of the stator at the (k+1) sampling period. The current predictions in equations (36,37) have seven different values for each of the seven voltage states that are presented in Table 1, the cost function [14] is computed for each time step, and MPC will solve the optimization problem, and the voltage vector that gives the minimum value of the cost function will be applied to the next sampling period. However, the future reference current value $i_{sdq}^{*}[k+1]$ is unknown. Therefore, it must be predicted from the present and the past. Values of the current reference by Lagrange extrapolation are as follows:

(41) $$i_{sdq}^{*}[k+1] = 3i_{sdq}^{*}[k] - 3i_{sdq}^{*}[k-1] + i_{sdq}^{*}[k-2]$$

4.2 MPC model in grid side converter

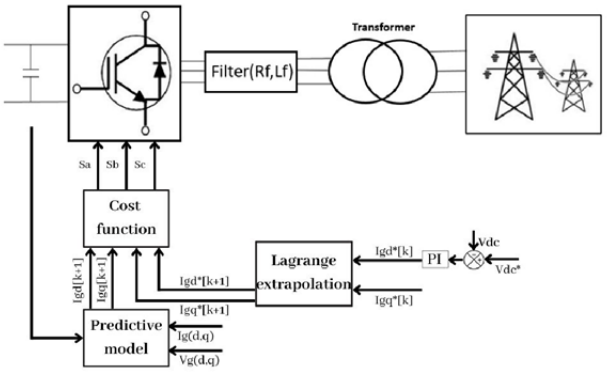

Fig.5. Grid side of PMSG wind turbine control system

The main objective of MPC GSC is to control the active and reactive power of the grid by controlling the grid current in the d-q frame, i_{gd}^{*} is computed via an external PI controller that regulates the voltage measured in the DC-link to track its reference at a constant value and i_{gq}^{*} is also computed via an external PI controller that regulates the reactive power to zero. We apply the forward Euler discretization method to equations (12,13), and the following prediction equations are obtained [12]:

(42) $$i_{gd}[k+1] = b_1 i_{gd}[k] + b_2 i_{gq}[k] + b_3(V_{gd}[k] - V_{id}[k])$$

(43) $$i_{gq}[k+1] = b_1 i_{gq}[k] - b_2 i_{gd}[k] + b_3(V_{gq}[k] - V_{iq}[k])$$

Where $b_1 = \frac{1-R_f T_s}{L_f}$, $b_2 = \omega_g T_s$, $b_3 = \frac{T_s}{L_f}$, $a_4 = -\frac{\omega_s T_s}{L_{sq}}$, and T_s is the sampling period. $i_{gd}[k+1]$ and $i_{gd}[k+1]$ are the grid predicted current in the dq frame at the (k+1) sampling period and $i_{gd}[k]$ and $i_{gd}[k]$ are the grid current in the dq frame at the (k) sampling period. Then a cost function in GSC is defined as follows [13]:

(44) $$g = \Delta i_{gd}[k+1] + \Delta i_{gq}[k+1]$$

With:

(45) $$\Delta i_{gd}[k+1] = (i_{gd}^{*}[k+1] - i_{gd}[k+1])^2$$

(46) $$\Delta i_{gq}[k+1] = (i_{gq}^{*}[k+1] - i_{gq}[k+1])^2$$

With $i_{gd}^{*}[k+1]$ and $i_{gq}^{*}[k+1]$ are the d-q axis reference stator current at the (k+1) sampling period, and they are obtained using Lagrange extrapolation:

(47)
$$i_{gdq}^{*}[k+1] = 3i_{gdq}^{*}[k] - 3i_{gdq}^{*}[k-1] + i_{gdq}^{*}[k-2]$$

Table 1. State of switch and corresponding voltage output

S_a	S_b	S_c	V_{sa}	V_{sb}	V_{sc}	V_j	V_{sdq}^{j}	V_{idq}^{j}
0	0	0	0	0	0	V_0	V_{sdq}^{0}	V_{idq}^{0}
1	0	0	$2V_{dc}/3$	$-V_{dc}/3$	$-V_{dc}/3$	V_1	V_{sdq}^{1}	V_{idq}^{1}
1	1	0	$V_{dc}/3$	$V_{dc}/3$	$-2V_{dc}/3$	V_2	V_{sdq}^{2}	V_{idq}^{2}
0	1	0	$-V_{dc}/3$	$2V_{dc}/3$	$-V_{dc}/3$	V_3	V_{sdq}^{3}	V_{idq}^{3}
0	1	1	$-2V_{dc}/3$	$V_{dc}/3$	$V_{dc}/3$	V_4	V_{sdq}^{4}	V_{idq}^{4}
0	0	1	$-V_{dc}/3$	$-V_{dc}/3$	$2V_{dc}/3$	V_5	V_{sdq}^{5}	V_{idq}^{5}
1	0	1	$V_{dc}/3$	$-2V_{dc}/3$	$V_{dc}/3$	V_6	V_{sdq}^{6}	V_{idq}^{6}
1	1	1	0	0	0	V_7	V_{sdq}^{7}	V_{idq}^{7}

5. Simulation results and discussion

This section presents a simulation of the proposed model predictive control with sliding mode control using the MATLAB/Simulink environment for evaluating its performance in a dynamic regime. The wind speed used in the simulation ranges from 5 m/s to 15 m/s for 10 s, as presented in figure 6. The SMC was then compared with the proposed MPC. Finally, a robustness test was performed for the MPC by varying the system parameters. The basic simulation parameters are listed in Tables 2, 3, 4, and 5.

Table 2. Parameters of PMSG

Symbol	Value
Rated power P_m	2 MW
Nominal voltage	5000 V
Stator resistance R_s	0.00625 Ω
Stator direct inductance L_{sd}	0.004229 H
Stator quadrature inductance L_{sd}	0.004229 H
The moment of inertia J	10000 $Kg.m^2$
The friction coefficient f	0.0142 $N.m$
Pole pairs P	75

Table 3. Parameters of wind turbine

Symbol	Value
Blade length R	55 m
Air density ρ	1.225 Kg/m^3
Gain multiplier G	1

Table 4. Parameters of the grid

Symbol	Value
Filter resistance R_f	0.002 Ω
Filter inductance L_f	0.004 H
Fixed-step size T_s	1e-5

Table 5. Parameters of SMC

Symbol	Value
Gain K_{mec}	7000
Gain K_{sd}	20
Gain K_{sq}	30
Gain K_{gd}	100
Gain K_{gq}	300

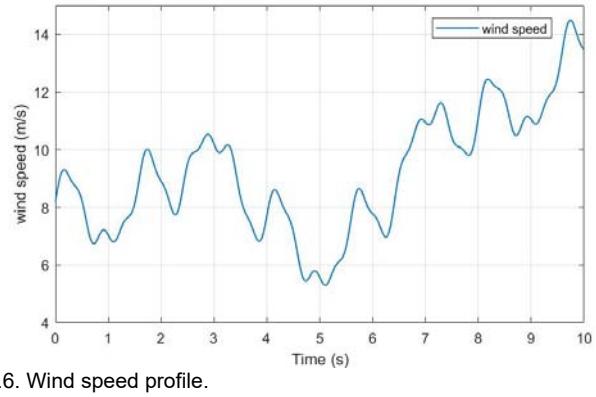

Fig.6. Wind speed profile.

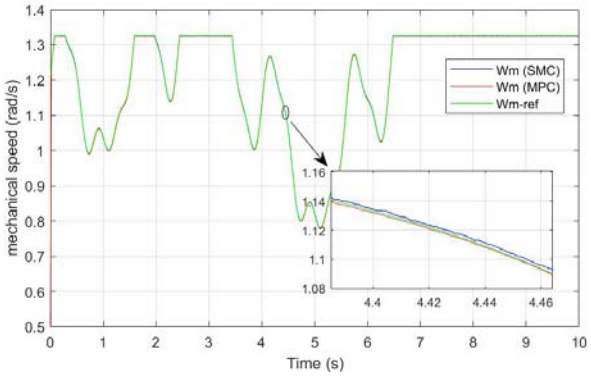

Fig.7. Mechanical speed.

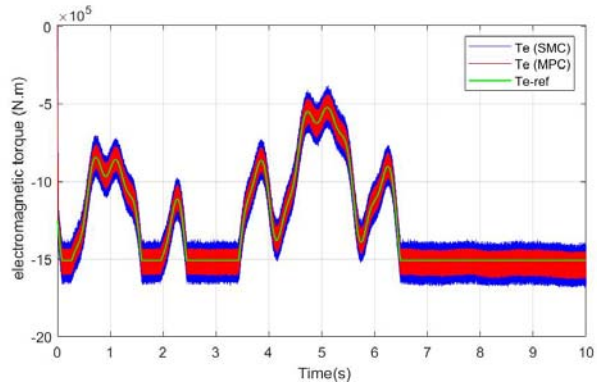

Fig.8. Electromagnetic torque.

We can notice from figure 7 that the mechanical speed is the image of the wind profile when speed is below 9 m/s, but if the wind accedes this speed, then pitch control will limit the output power of the wind turbine to 2MW hence limiting all the variables including mechanical speed, turbine torque for security reasons. Fig.8 shows that the electromagnetic torque follows its reference imposed by the MPPT technique, extracting the maximum wind energy available.

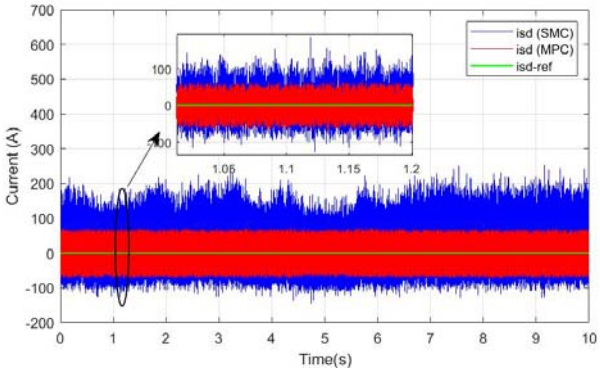

Fig.9. D-axis stator current.

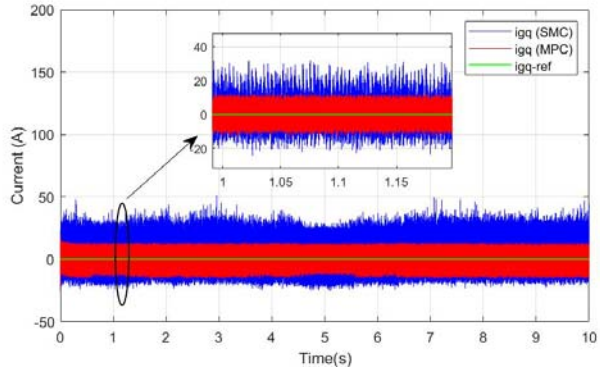

Fig.10. Q-axis grid current.

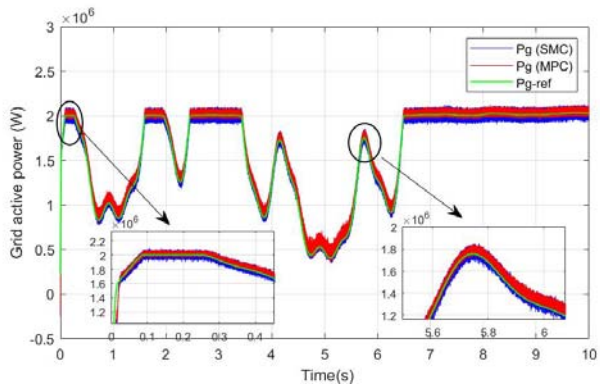

Fig.11. Grid active power.

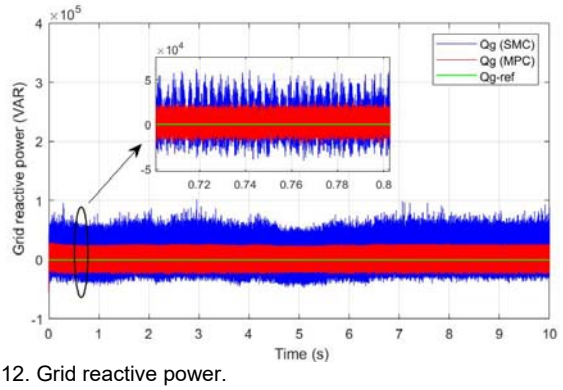

Fig.12. Grid reactive power.

figure 9 and figure 10 present the stator d axis current and grid q axis current that is maintained at the value of zero, we can notice from both figures that the SMC technique has the disadvantage of chattering, which is noise in our signal, but our proposed technique controls both current in an optimal way fixing the chattering problem.

From figure 11, we note a fast response in the grid active power of the two controls used, but MPC offers a better control because of its accuracy. Fig.12 shows the reactive power controlled by both techniques to maintain the value zero to achieve a unit power factor. SMC again offers a fast response yet fails against MPC regarding chattering.

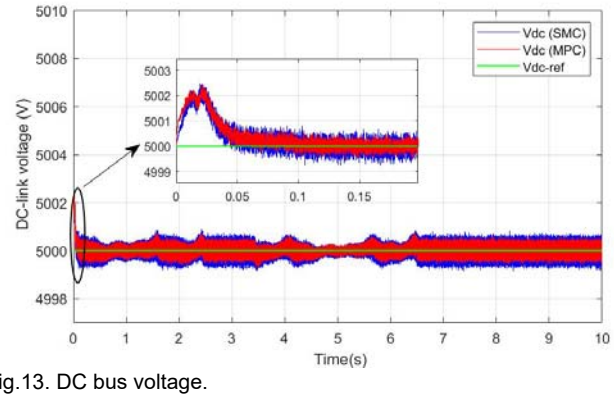

Fig.13. DC bus voltage.

Fig.13 Shows the DC bus voltage with both controls, as we notice both controls work fine with no issues, but MPC offers lower errors.

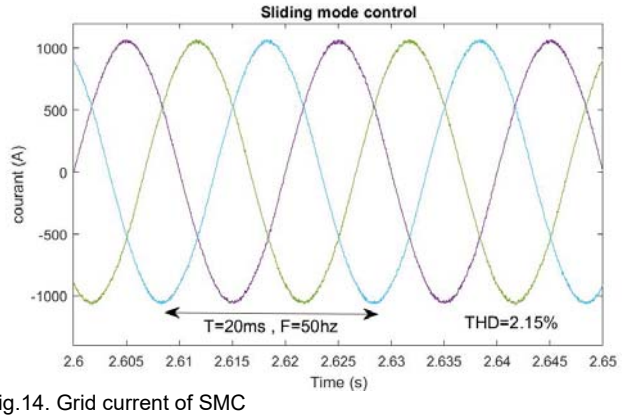

Fig.14. Grid current of SMC

As can be seen in figures 14 and 15, the amplitude of the injected current changes according to the wind profile, and both controls offer a suitable sinusoidal waveform with a fixed frequency of 50 Hz; we performed a harmonic analysis to study the current quality fed to the grid, we notice a lower THD with the MPC than with the SMC.

The MPC's robustness [15] was tested by varying the system resistance and inductance, doubling the stator resistance, increasing the stator d-q inductance by 25%, doubling the filter resistance, and decreasing the filter inductance by 25%. figure 12 presents the effect of varying the parameters on the grid current waveform and its quality.

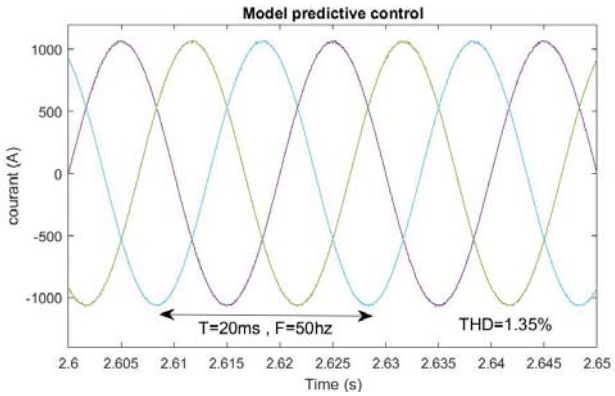

Fig.15. Grid current with MPC.

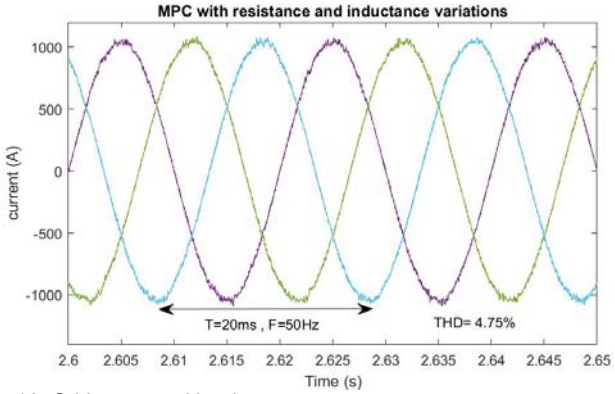

Fig.16. Grid current with robustness test.

Figure 16 shows the robustness test shows an increased THD compared to the first test, which is expected considering the variations, therefor we can say MPC can handle parameter variations and unexpected variations to the system.

6. Conclusion

In this paper, we have controlled a PMSG based on wind energy using Model Predictive Control and compared the obtained results in the same wind condition using Sliding Mode Control , both of them are advanced controls, but although SMC is considered one of the best controls because of its efficiency and its robustness but one of the challenges it's the phenomenal of chattering, There for we proposed the predictive control based on the model of the system which correct this disturbing outstanding, The mathematical model of the system including the wind turbine has been established at first, then both controls have been synthesized. The results show that MPC offers better current control with a better sinusoidal waveform of the grid injected current and a lower THD compared to SMC with the chattering phenomenal.

Table 6. Performance comparison between SMC and MPC

Performance	SMC	MPC
Cosphi	99.99%	99.98%
Overshoot V_{dc}	0.0528	0.0430
Variation band of Q_g(KVAR)	118.5	33.3
THD of injected current	2.15%	1.35%
THD with robustness test	3.04%	4.75%
Robustness	High	High

***Authors**:*
***Dr. Abdallah BELABBES**, University of Science and Technology MB, Laboratory of Vision Automation and Intelligent Control Systems AVCIS, Bir El Djir, 31000 Oran, Algeria E-mail: abdallah.belabbes@gmail.com;*
***Anouar LAIDANI**, University of Oran 2, Industrial maintenance and safety institute, Bir El Djir, 31000 Oran, Algeria E-mail: Laidaninoanoir@gmail.com;*
***Amina YACHIR**, National Polytechnic School, Laboratory of Automation and Systems Analysis LAAS, Route d'Es-Sénia, Oran, Algeria, E-mail: amina.inge@yahoo.fr;*
***Dr. Allal El Moubarek BOUZID**, Icam, site de Toulouse, France, E-mail: allal.bouzid@icam.fr;*
***Dr. Riyadh BOUDDOU**, Department of Electrical Engineering, Institute of Technology, University Center of Naama, Algeria, E-mail: bouddou@cuniv-naama.dz;*
***Omar Abdelaziz LITIM**, University of Oran 2, Industrial maintenance and safety institute, Bir El Djir, 31000 Oran, E-mail: litimomarabdelaziz@gmail.com;*

REFERENCES

[1] BOSSOUFI, Badre, KARIM, Mohammed, TAOUSSI, Mohammed, et al. DSPACE-based implementation for observer backstepping power control of DFIG wind turbine. IET Electric Power Applications, 2020, vol. 14, no 12, p. 2395-2403.

[2] BENAMOR, A., BENCHOUIA, M. T., SRAIRI, K., et al. A novel rooted tree optimization apply in the high order sliding mode control using super-twisting algorithm based on DTC scheme for DFIG. International Journal of Electrical Power & Energy Systems, 2019, vol. 108, p. 293-302.

[3] SENTURK, Osman S., HELLE, Lars, MUNK-NIELSEN, Stig, et al. Power capability investigation based on electrothermal models of press-pack IGBT three-level NPC and ANPC VSCs for multimegawatt wind turbines. IEEE Transactions on Power Electronics, 2012, vol. 27, no 7, p. 3195-3206.

[4] REYES-LÚA, Adriana et SKOGESTAD, Sigurd. Systematic design of active constraint switching using classical advanced control structures. Industrial & Engineering Chemistry Research, 2019, vol. 59, no 6, p. 2229-2241.

[5] Laidani, A., Litim, Commande avancé d'une Génératrice synchrone à aimant permanent intégré dans un système éolien Memory for graduation master in *University of Oran 2, Industrial maintenance and safety institute* University Mohamed Ben Ahmed Oran 2, July 2023.

[6] EMNA, Mahersi Emna, KHEDER, A. D. E. L., et MIMOUNI, Mohamed Faouzi. The wind energy conversion system using PMSG controlled by vector control and SMC strategies. International Journal of Renewable Energy Research, 2013, vol. 3, no 1, p. 41-50.

[7] MEKKI, Mustapha, ALLAOUI, Tayeb, BELABBAS, Belkacem, et al. Decoupling vector control and optimisation of PMSG-based wind energy system using adaptive type-1 and type-2 fuzzy logic control. Przegląd Elektrotechniczny, 2020, vol. 96.

[8] SAIDI, Youcef, MEZOUAR, Abdelkader, MILOUD, Yahia, et al. Modeling and adaptive power control-designed based on tip speed ratio method for wind turbines. Przegląd Elektrotechniczny, 2019, vol. 95, no 6, p. 40-46.

[9] GHOURAF, Djamel Eddine. An advanced control applied to PMSG wind energy conversion system implemented under graphical user interface. Electrical Engineering, 2023, p. 1-12.

[10] KOUMBA, Paul Makanga, CHERITI, Ahmed, DOUMBIA, Mamadou Lamine, *et al.* Wind turbine control based on a permanent magnet synchronous generator connected to an isolated electrical network. In : *2017 IEEE Electrical Power and Energy Conference (EPEC)*. IEEE, 2017. p. 1-7.

[11] FAEDO, Nicolás, OLAYA, Sébastien, et RINGWOOD, John V. Optimal control, MPC and MPC-like algorithms for wave energy systems: An overview. IFAC Journal of Systems and Control, 2017, vol. 1, p. 37-56.

[12] SRIVASTAVA, Apoorva et BAJPAI, R. S. Model predictive control of grid-connected wind energy conversion system. IETE Journal of Research, 2022, vol. 68, no 5, p. 3474-3486.

[13] HASSINE, Ikram Maaoui-Ben, NAOUAR, Mohamed Wissem, et MRABET-BELLAAJ, Najiba. Predictive control strategies for wind turbine system based on permanent magnet synchronous generator. ISA transactions, 2016, vol. 62, p. 73-80.

[14] CORTÉS, Patricio, KAZMIERKOWSKI, Marian P., KENNEL, Ralph M., et al. Predictive control in power electronics and drives. IEEE Transactions on industrial electronics, 2008, vol. 55, no 12, p. 4312-4324.

[15] TOUMI, Sana, ELGHALI, SE Ben, TRABELSI, Mohamed, et al. Robustness analysis and evaluation of a PMSG-based marine current turbine system under faulty conditions. In : 2014 15th International Conference on Sciences and Techniques of Automatic Control and Computer Engineering (STA). IEEE, 2014. p. 631-636.

[16] BELABBES, A., HAMANE, B., BOUHAMIDA, M., *et al.* Power control of a wind energy conversion system based on a doubly fed induction generator using RST and sliding mode controllers. In : *International Conference on Renewable Energies and Power Quality*. 2012.